Accurate Characterization of Radiation from Interconnects on Interposer at mmWave Frequencies

Martijn Huynen, Dries Bosman, Arno Moerman and Dries Vande Ginste
quest, Department of Information Technology, Ghent University/imec, Belgium
www.questlab.be
martijn.huynen@ugent.be

***Abstract*—An electromagnetic interference (EMI) assessment of mmWave interposers becomes increasingly important as the need for heterogeneous systems increases. However, the small size and complexity of these platforms make it more difficult to accurately measure them and, thus, a dedicated set-up to isolate the interposer's emission is required. In this contribution, we first show experimentally that at mmWave frequencies surface waves originating on the interposer test vehicles may interact with the larger measurement board and severely impact the radiation pattern and maximum electric field strength. Second, a simulation study into the exact origins confirms these surface waves indeed to be at the heart of this issue and calls for appropriate measures in interposer design to prevent any EMI complications when integrating this component in a larger system.**

***Index Terms*—mmWave measurement, interposer design, interconnect, EMI assessment**

I. Introduction

Next generation communication technologies are unceasingly being developed to cope with the trend towards a densely interconnected environment. Combined with the demand for increased quality, reduced latency and large bandwidth, engineers and designers are pushing the boundaries on all fronts to pave the way for novel communication applications. One such facet is the evolution towards millimeter wave (mmWave) frequencies as the main bands for telecommunication systems. This rise in frequency does of course not come freely; it brings along many challenges in terms of propagation environment and absorption peaks but also has an impact on the hardware level. Higher operation frequencies pose challenges for the efficiency of active and passive components, which, in combination with the continuing miniaturization, leads to ever more complex interconnects. Consequently, considering the tendency for heterogeneous systems, a state-of-the-art interposer becomes a vital building block in the overall system.

An interposer's complex nature and mmWave operation/capability impose stringent electromagnetic compatibility (EMC) requirements on its design. Not only is it imperative that the signal integrity (SI) of the subsystems placed on the interposer remains guaranteed, the signal lines on the interposer itself can also be of substantial electric length and thus start to behave as effective radiators [1]. Given the composite nature of an interposer-based system and the resulting complex signal interplay, it becomes increasingly difficult to locate and mitigate all potential electromagnetic interference (EMI) appropriately.

In light of these challenges, we conducted a study into interconnect structures on interposer to identify all radiation mechanisms during measurements of dedicated test vehicles. Accurately measuring interposers' radiation at mmWave frequencies is no simple feat as their size becomes small compared to typical fixtures, connectors, cables and equipment found in an electromagnetic anechoic chamber, leading to an increasing influence of the measurement set-up on the captured results. To assess the feasibility of such interposer measurements, we designed several test structures around $30\,\mathrm{GHz}$ and devised a measurement set-up to isolate the interposer's radiation to the full from any unwanted influence.

In this contribution we start by presenting the mmWave test vehicles and the thought process behind the measurement set-up. Afterwards, we describe the measured radiation patterns and try to isolate the dominating contributions, which involves a short simulation study to find the cause of the observed discrepancy between simulated and measured results. The origin of these differences turns out to be the excitation of surface waves, interacting with the larger ground plane of the printed circuit board, which was required in the measurement set-up. We conclude with some recommendations to mitigate the encountered difficulties in this campaign and outline future work that would lead to additional insight into the matter.

II. Measurement of test vehicles

The test vehicles are all realized on a six layer interposer with HL972LF (LD) ($\epsilon_r = 3.4$ and $\tan\delta = 0.004$) as a core and prepreg material, and copper for the metal layers. As all structures exhibit features solely on the top and bottom metal layers of thickness $15\,\mu\mathrm{m}$ with vias passing through the entire stack-up of $600\,\mu\mathrm{m}$, these dimensions suffice for a full description in this application. The fabricated test vehicles are shown with annotated dimensions in Fig. 1. They are an inset-fed patch antenna, a straight microstrip and a microstrip with 90° bend, respectively, and are all situated on their separate $10\,\mathrm{mm} \times 10\,\mathrm{mm}$ interposer. Feeding is realized by a via through the full substrate to provide optimal shielding.

Although it is not typically found on an interconnect interposer, the patch antenna is included as our primary test structure for two main reasons. First, the antenna acts as a strong radiator with a well-known, clear radiation pattern and thus fulfills the role of a calibration structure to evaluate the

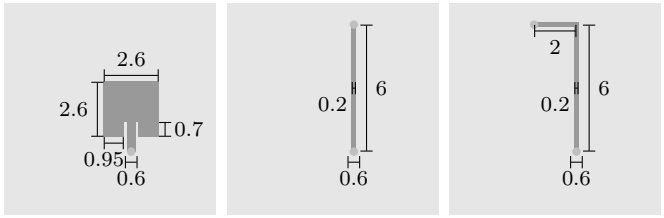

(a) Patch antenna. (b) Straight microstrip. (c) Line with right-angled bend.

Fig. 1. Interposer test vehicles. All annotated dimensions are given in mm.

similarity between simulation and measurement results. Second, the resonant nature of the antenna and dependency of its resonance frequency on both substrate thickness and dielectric constant enable us to quickly detect any discrepancy between the designed structures and their fabricated counterparts and adjust the analysis accordingly.

The remaining structures are basic interconnects, viz., a straight microstrip of length 6 mm and a microstrip with a 90° bend where the two line segments measure 6 mm and 2 mm, respectively. Both lines are fabricated in two variants: one where the top end is shorted to ground and another where that side can be routed through and connected to a 50 Ω load.

Given the relatively small size of the interposers compared to the cables and measurement fixtures or even the employed connectors (Southwest Microwave End Launch K connectors), a larger PCB was required (4 cm × 6.5 cm) to comfortably accommodate the connectors and fix the test vehicles to the positioning system, which constitutes the NSI-700S-30 Spherical near-field and far-field system, equipped with an open ended waveguide probe in the appropriate band. This larger measurement PCB has a total thickness of 1 mm and is comprised of 6 metal layers of Megtron6 ($\epsilon_r = 3.4$ and $\tan\delta = 0.004$) substrate. However, care had to be taken as the larger PCB's emission could easily trump the radiation of the interposers. Therefore, we utilized a similar strategy as on the interposer: the feed line is implemented on the bottom layer of the PCB and the signal is brought to the top layer by a through via while all other layers are grounded. The interposer and PCB are interconnected by means of a 10 × 10 ball grid array in such a way that every signal connection is surrounded by 8 grounded neighbors, minimizing any radiation from the ball grid. The feed line on the board is realized in a GCPW topology, further suppressing its inherent emission.

In terms of the set-up in the full anechoic chamber further measures were taken to reduce interference from the measurement infrastructure. First of all, the cable running from the rotary joint to the PCB connector is connected to the board's side with a right-angled adapter to minimize any primary emission contribution from the cable to the radiation pattern. Furthermore, all exposed metal and cables are shielded as good as possible with additional (pyramidal) electromagnetic absorbers. Calibration of the measured realized gain is accomplished by a reference assessment with a WR-34 standard gain horn and the loss of the PCB's feed line is estimated through a TRL calibration set.

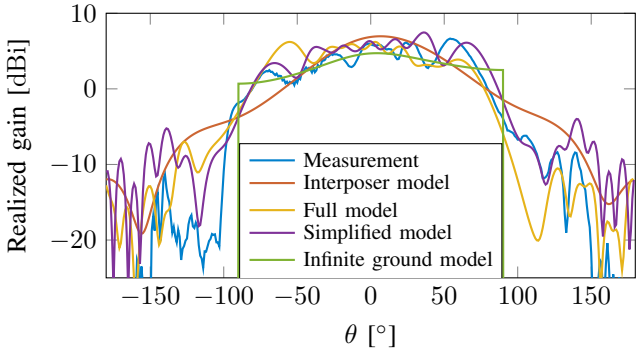

Fig. 2. Realized gain of the patch antenna in a $\phi = 90°$ cut at 28 GHz for the measurement and various simulation models.

III. Results

Before looking at the radiated emission of the test structures, we checked the reflection coefficient of the assembled patch antenna to detect any potential resonance shift. In the simulation model, the patch resonates at 29 GHz while its fabricated counterpart exhibits a dip in the S-parameter magnitude around 28 GHz, thus indicating a deviation in the stack-up. To compensate for this frequency disparity, we will shift the simulation results in the remainder of this paper down by 1 GHz when looking at radiation characteristics.

As mentioned before, we utilize the patch antenna as a reference structure since it is intended to be employed as a strong radiator. Fig. 2 displays the radiation pattern of the realized gain in a $\phi = 90°$ cut, i.e., along the feed line of the antenna, at 28 GHz for the measured data and for different simulation models obtained via CST Microwave Studio. The gain pattern of the simulated interposer on its own (red line) demonstrates the typical main lobe of a microstrip patch antenna. The measured pattern (blue curve) displays a similar maximum gain at $\theta = 0°$ with a broadened beam and suppressed back radiation due to the PCB's large ground plane. However, the most striking, and in first instance somewhat unexpected, feature of the measured data is the prominent ripple superimposed on the otherwise smooth gain pattern of the patch antenna. A simulation of the full device (yellow line), i.e., interposer, BGA, PCB and connector, reveals that the phenomenon is not a fluke but the result of an electromagnetic interaction between the components.

The following short simulation study reveals that the root cause of this ripple are surface waves excited on the interposer and which interact with the electrically large ground plane of the PCB. Surface or Sommerfeld-Zenneck waves are bounded cylindrical waves that can exist at interfaces between two media with different dielectric constants [2]. Typically they are classified in modes, analogously to waveguide modes, with the main types transverse electric (TE) and transverse magnetic (TM) modes. The cut-off frequencies of these modes can be calculated analytically for the simple stack-up of the interposer [3]. The lowest TE mode has a cut-off frequency around 77 GHz and thus cannot be the origin of the ripple. However, the lowest TM mode can be supported at any frequency and since it has a vertical electric component, it could easily be excited by, e.g., vias through the substrate.

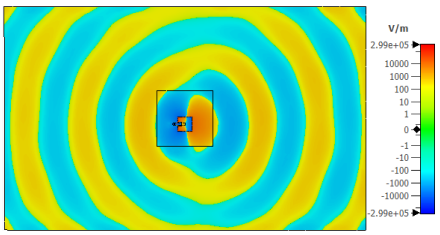

Fig. 3. Normal electric field distribution at 28 GHz on the simplified simulation model. The surface waves are clearly generated on the interposer and interact strongly with the electrically large ground plane.

Yet, the presence of a via does not necessarily imply the occurrence of an unwanted ripple due to surface waves. As discussed earlier, the simulation model of the interposer on its own shows no ripple at all (see Fig. 2). The other edge case, where the interposer is backed by an infinitely large ground plane (green curve), can be seen in the same figure too. The ground plane drastically alters the gain pattern: it is broadened and exhibits a reduced maximum gain but nonetheless remains smooth. The ripple is only observed when an electrically large, albeit finite, ground plane is added to the back of the interposer. This is also demonstrated in the purple curve on Fig. 2, which corresponds to the isolated interposer model with its ground plane (but not substrate) size increased to that of the PCB. This simplified model reveals the same ripple effect as the full blown model (in yellow) but simulates faster as it does not take all the details of the PCB into account. Fig. 3 shows the electric field for this simplified model and clearly demonstrates the excited surface waves at the patch antenna, propagating on and interacting with the electrically large ground plane, eventually leading to the ripple in the gain.

The ripple on the gain pattern does not solely occur for the antenna test vehicle but can also be observed on two interconnect examples. In Fig. 4, the same $\phi = 90°$ cut of the radiation pattern at 28 GHz is shown as before, together with the results from various simulation models.

In an EMC context, a decisive quantity to assess a system's radiated emission performance is not so much the complete radiation pattern as the maximum electric field strength at a fixed distance. Here we opt to compute this value at 3 m, scaled for a power of 1 W at the input port of all structures.

In Figs. 5–9 this measure is shown for the five test vehicles, the patch antenna, shorted microstrip, shorted microstrip with right angle, matched microstrip and matched microstrip with right angle, respectively. For each interposer the fields were measured and simulated from 25 GHz to 32 GHz. For the patch antenna, all simulation models differ no more than 2 dB from the measurement results. The largest discrepancy is observed for the simplified model where the lack of loss mechanisms in the PCB seems to lead to a structural overestimation of the large ground plane's effect. For this strong radiator, a comparison between the full and interposer-only model shows remarkably little deviation and a very close agreement to the measured data. The reduction in maximum gain at $\theta = 0°$ due to the ground plane appears to be compensated almost perfectly by the ripple on the radiation pattern in terms of maximum field strength.

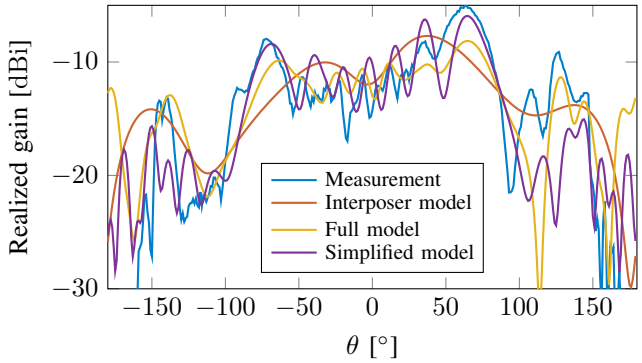

(a) Shorted microstrip line.

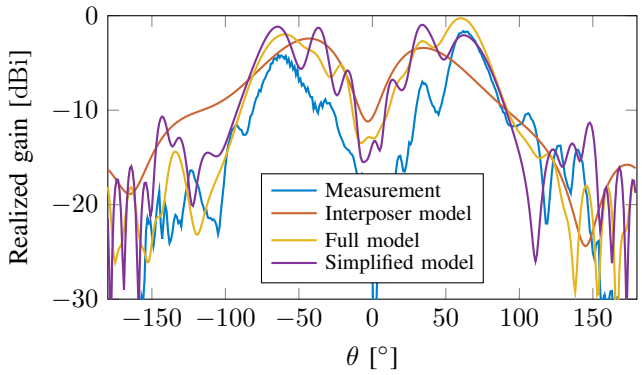

(b) Shorted microstrip with bend.

Fig. 4. Realized gain of the two interconnect test vehicles in a $\phi = 90°$ cut at 28 GHz for the measurement and various simulation models.

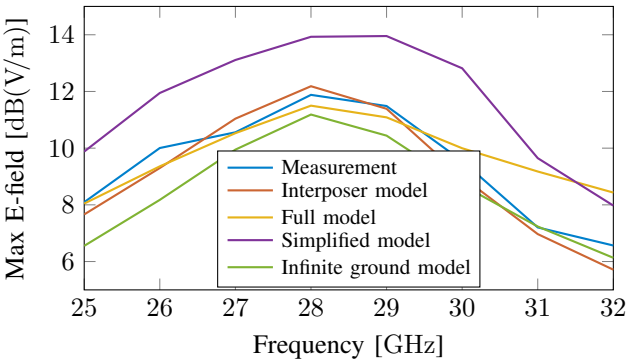

Fig. 5. Maximum electric field value at 3 m for an input power of 1 W for the microstrip patch antenna.

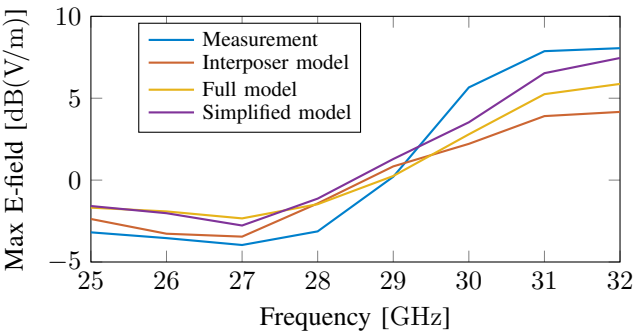

Fig. 6. Maximum electric field value at 3 m for an input power of 1 W for the shorted straight microstrip.

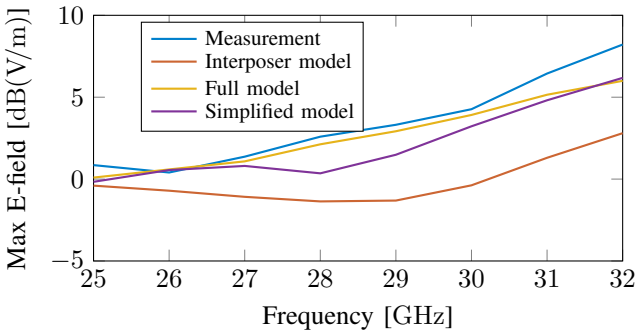

Fig. 7. Maximum electric field value at 3 m for an input power of 1 W for the matched straight microstrip.

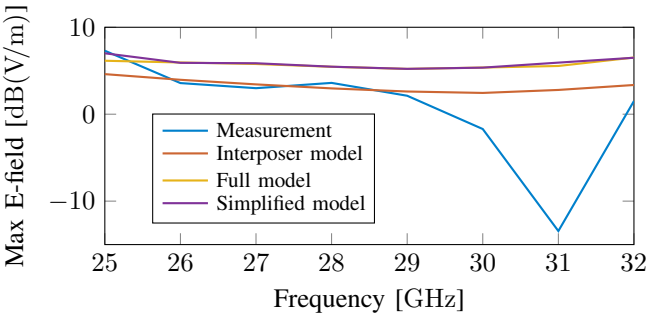

Fig. 8. Maximum electric field value at 3 m for an input power of 1 W for the shorted microstrip with right angle.

The same conclusion does not hold up for the interconnect structures. Here, a clear difference between the interposer model and the simplified or full assembly model is discerned. For the straight microstrip (Figs. 6–7) the larger simulation models predict the measured field levels better, following the trend over the observed frequency range and staying within 2 dB of the measured curves. The interposer model, contrarily, tends to underestimate the measure by as much as 6 dB, in particular at the higher frequency end. It is also interesting to note that for these interconnect examples, the difference between the full PCB model and the simplified simulation set-up is much smaller, indicating that the ripple effect has a larger impact for these lines than it does for the patch antenna.

For the microstrip lines with right-angled bend, the same comparison between the included simulation models can be drawn (Figs. 8–9). However, above 29 GHz, the measured data starts deviating quite strongly from all simulation models for these structures. The test vehicles exhibit a very strong

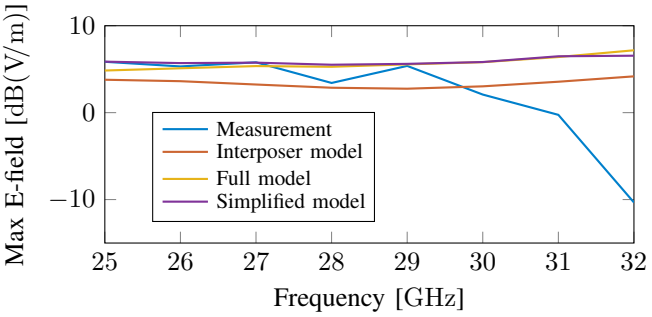

Fig. 9. Maximum electric field value at 3 m for an input power of 1 W for the matched microstrip with right angle.

dip in radiation around 31 GHz that has not been replicated in any simulation model. Despite various tests, both on the fabricated structures and in simulation, we have not been able to decisively pinpoint the cause of this phenomenon, although an unidentified mismatch issue seems to be the most likely cause. Nevertheless, the large simulation models predict the field levels best for the matched line with bend while the interposer model does this better for the shorted line at frequencies below 29 GHz.

IV. Conclusion

In this work, the properties of five mmWave test vehicles were studied through simulation and measurement, to identify the dominant radiation contributions in typical interconnect structures on interposers. A modeling strategy was devised to efficiently yet still accurately predict the pertinent characteristics and a meticulously constructed measurement set-up prevented perturbation of the results by external factors. We demonstrated that due care must be taken when designing and applying interposers, to avoid the unwanted excitation of surface waves, influencing the maximally emitted electric field and thus potentially jeopardizing EMC compliance of the considered device. In particular, if an interposer is positioned on a (typically larger) PCB, the interaction of such surface waves with its ground plane might enforce preventive measures and simplified simulation models of the interposer only might underestimate the emitted radiation by up to 6 dB.

Therefore, it is imperative to suppress or even completely eliminate the excitation of these unwanted waves. Carefully designing and shielding of vertical via transition appears to be a crucial procedure as such structures were identified as the main source. However, the choice in interconnect topology itself is paramount as well since lines realized as a (grounded) coplanar waveguide or a stripline are better suited to confine excited surface waves. For antennas realized on interposer, cavity backed designs are a solution to limit the influence of surface waves on the performance [4].

Since interconnect structures are often conceived with a differential topology, an exploration into such examples might reveal additional relevant guidelines and provide more insight into the topics we treated here. In particular, the distinction between common mode and differential mode components in the occurring signals should be made as they will inherently influence the excitation of surface waves.

V. Acknowledgments

The authors would like to thank dr. Zhao Caijun and his team at Huawei for inspiring these designs and line of research.

References

[1] M. Swaminathan, K. J. Han , *Design and modeling for 3D ICs and interposers*. World Scientific, 2013.
[2] J. G. Van Bladel , *Electromagnetic Fields*. John Wiley & Sons, 2007.
[3] C. A. Balanis , *Advanced Engineering Electromagnetics, 2nd Edition*. Wiley, 2012.
[4] I. Lima de Paula, S. Lemey et al. , "Cost-Effective High-Performance Air-Filled SIW Antenna Array for the Global 5G 26 GHz and 28 GHz Bands," *IEEE Antennas and Wireless Propagation Letters*, vol. 20, no. 2, 2021, pp. 194–198.